

Research Article

Comparison of Performance of Photodiodes with Different Active Areas Using Acrylic and Quartz Cuvettes for Spectrophotometry in Direct Measurements of Glucose in Water and Human Blood Plasma by Optical Means Using Near-Infrared

Victor De La Cruz Cortes , Kristian Segura Félix , Francisco Gerardo Flores García ,
and Mario Francisco Jesús Cepeda Rubio 

División de Estudios de Posgrado e Investigación, Instituto Tecnológico de La Laguna, Torreón 27274, Coahuila, Mexico

Correspondence should be addressed to Francisco Gerardo Flores García; fgfloresg@correo.itlalaguna.edu.mx

Received 29 September 2021; Accepted 4 January 2022; Published 4 February 2022

Academic Editor: Jau-Wern Chiou

Copyright © 2022 Victor De La Cruz Cortes et al. This is an open access article distributed under the Creative Commons Attribution License, which permits unrestricted use, distribution, and reproduction in any medium, provided the original work is properly cited.

Diabetes mellitus is one of the most relevant noncommunicable diseases; the WHO figures in its latest update that 422 million people suffer from it; additionally, it has remained for more than 20 years within the 10 main causes of death worldwide; this disease affects the population at any age; glucose measurement is used to assist the treatment of this disease by different methods that are classified as invasive, minimally invasive, and noninvasive, the latter being an area of recent development due that it is not traumatic for patients. This work consists of the experimental characterization of an optical system for plasma glucometry using near infrared by spectrophotometry. This glucometry system is based on the employ of an infrared LED with a wavelength of 1650 nm, a beam angle of 16°, and an output power of 1.6 mW that passes through the analyte (glucose in blood plasma) that is contained in cuvettes of different materials (acrylic and quartz) to subsequently affect a photodiode with different active areas ranging from 0.06 mm to 1.5 mm in order to evaluate the efficiency by comparing the sensitivity in the presence of glucose making additions ranging 100 mg/dl–1000 mg/dl within a dark chamber. The experiments showed that the use of photodiodes with a larger active area and the use of quartz cuvettes show a higher sensitivity compared to photodiodes with small active areas and the use of acrylic cuvettes. This configuration presented an R^2 of 0.99 and a sensitivity of 0.225 mV/1 mg/dl of glucose; despite the fact that the initial voltage in each of the experimental repetitions varies, the downward voltage pattern is maintained; based on this, it is concluded that this method using this setup is feasible for plasma glucose measurement.

1. Introduction

According to the WHO, 422 million people suffer from diabetes [1]. It is considered one of the 4 most common noncommunicable diseases [2]. This disease triggers a set of metabolic disorders, which makes the patient's body unable to regulate glucose levels in blood. Some symptoms are increased thirst and urination, fatigue, blurred vision, slow-healing sores, and frequent infections. There are two basic types of diabetes: type 1, which generally occurs in adolescents and children, although it can manifest at any age, and type 2 is more common and affects mainly adults

[1, 3, 4]. It is estimated that by the year 2045, the number of cases will reach 629 million [5].

There are three techniques for measuring blood glucose: invasive, minimally invasive, and noninvasive. The invasive technique is by means of the extraction of a drop of blood having a high precision of measurement, for which it is very widely used. This technique is done by reacting a drop of blood with an enzyme. Depending on the type of the test strip used [6], the reaction of glucose with the enzyme generates electrons or a color change, which is then measured by an electronic device that converts it to glucose level [7].

The minimally invasive measurement technique consists of the application of a microneedle that is in contact with the interstitial fluid found in the skin. It is usually placed on the forearm, constantly monitoring glucose levels. This technique has the disadvantage of having a delay in the measurements due to the diffusion time of blood towards the interstitial liquid and having a very high cost [8].

The noninvasive glucose measurement technique often uses various methods such as infrared, photoacoustic, ultrasound, and fluorescence to detect glucose in blood. This technology has shown the feasibility of having precise measurements, with near-infrared spectroscopy being one of the most promising techniques [9].

The near infrared spectrometry technique uses Beer Lambert's law [10]; this technique measures the absorbance at a certain wavelength, the amount of glucose being proportional to the amplitude of the received signal. When there is a higher concentration of glucose, the emitted light will be absorbed by the glucose molecules, reducing the amplitude of said signal; this absorbance can be deduced from the measured glucose concentration [11].

In the present work, the use of near infrared spectroscopy is proposed, using an LED with a peak wavelength at 1650 nm as an emitting device and a photodiode as a receiver with a spectral range of 800–1700 nm for the measurement of glucose on human blood plasma. A comparison between the active area of the photodiode and the materials of the cuvette is carried out in order to know the ideal parameters to consider for the design of a noninvasive blood glucose meter.

2. Materials and Methods

An electronic prototype is used and mounted inside a small black box to isolate ambient light and obtain greater precision in measurements, as shown in Figure 1. The acquired signal is conditioned and processed by active amplifiers and filters to later proceed to its visualization and interpretation.

A multimeter BK precision 5491A was used to measure the voltage throughout the experiment.

Figure 2 shows the implemented system, where the physical elements used and their interrelationships and connections between each stage of the system are presented.

2.1. Glucose Samples in Tridistilled Water. 10 samples of glucose solutions were utilized in a range of 100–1000 mg/dl with an increment of 100 mg/dl. This range represents the concentrations of diabetic patients' blood glucose under various conditions. Blood consists of different constituents such as water, fats, proteins, triglycerides, cholesterol, and glucose among others, with water being the main and largest component [12]. Because of this, tridistilled water is ideal as a solvent on the samples of glucose solutions. The materials used in each solution were tridistilled water and solution DX-5, Pisa (glucose with concentration of 5000 mg/dl). The samples were made with the proportions given in Table 1 and according equations (1)–(5).

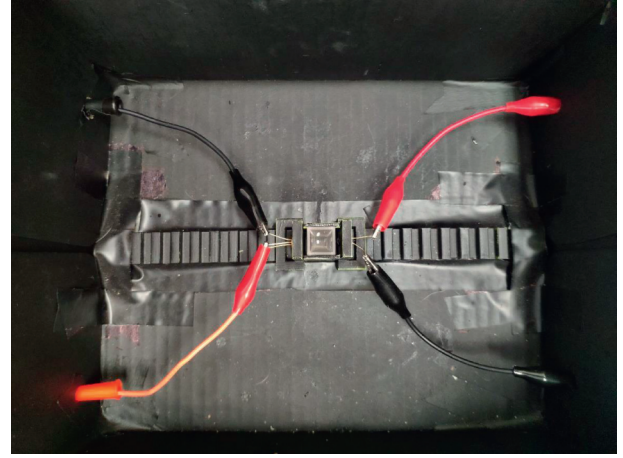


FIGURE 1: Prototype used for glucose measurement.

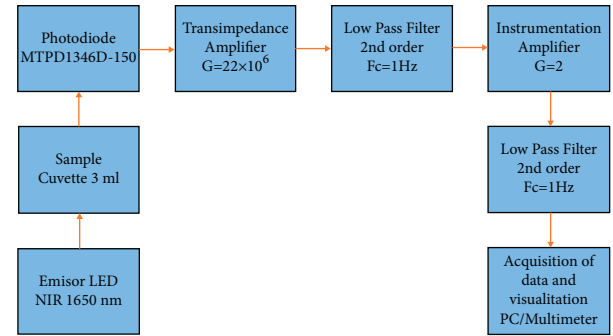


FIGURE 2: System block diagram.

TABLE 1: Concentrations used for preparing samples of glucose solutions.

Samples (mg/dl)	Tridistilled water (ml)	Solution DX-5, Pisa (μ l)
100	3	61.3
200	3	125
300	3	191.5
400	3	260.9
500	3	333.4
600	3	409.1
700	3	488.4
800	3	571.5
900	3	658.6
1000	3	750

$$0\text{mg/dl} = \frac{0\text{ mg}}{3\text{ ml}}, \quad (1)$$

$$5000\text{mg/dl} = \frac{3.065\text{ mg}}{0.0613\text{ ml}}, \quad (2)$$

$$\frac{0\text{ mg}}{3\text{ ml}} + \frac{3.065\text{ mg}}{0.0613\text{ ml}} = \frac{3.065\text{ mg}}{3.0613\text{ ml}} = 100.12\text{mg/dl}, \quad (3)$$

$$5000\text{mg/dl} = \frac{37.5\text{ mg}}{0.750\text{ ml}}, \quad (4)$$

$$\frac{0 \text{ mg}}{3 \text{ ml}} + \frac{37.5 \text{ mg}}{0.750 \text{ ml}} = \frac{37.5 \text{ mg}}{3.750 \text{ ml}} = 1000 \text{ mg/dl.} \quad (5)$$

2.2. *Glucose Samples in Blood Plasma.* Human blood plasma with a concentration of 100 mg/dl and Pisa, DX-5 solution, with a concentration of 5000 mg/dl are used. 2 tubes of 4 ml with EDTA anticoagulant are extracted to subsequently centrifuge blood at 4000 rpm for 15 minutes; then, blood plasma is extracted from the tubes and deposited in the 3 ml cuvette for later analysis, as shown in Figures 3 and 4.

10 glucose concentrations plasma with increments of 100 mg/dl were prepared from a human blood plasma sample of 100 mg/dl, adding glucose of the Pisa solution to get the required concentration. The samples were made with the proportions given in Table 2 and according equations (6)–(10).

$$100 \text{ mg/dl} = \frac{3 \text{ mg}}{3 \text{ ml}}, \quad (6)$$

$$5000 \text{ mg/dl} = \frac{3.125 \text{ mg}}{0.0625 \text{ ml}}, \quad (7)$$

$$\frac{3 \text{ mg}}{3 \text{ ml}} + \frac{3.125 \text{ mg}}{0.0625 \text{ ml}} = \frac{6.125 \text{ mg}}{3.0625 \text{ ml}} = 200 \text{ mg/dl,} \quad (8)$$

$$5000 \text{ mg/dl} = \frac{33.75 \text{ mg}}{0.675 \text{ ml}}, \quad (9)$$

$$\frac{3 \text{ mg}}{3 \text{ ml}} + \frac{33.75 \text{ mg}}{0.675 \text{ ml}} = \frac{36.75 \text{ mg}}{3.675 \text{ ml}} = 1000 \text{ mg/dl.} \quad (10)$$

2.3. *Glucose Measurement.* In this stage, an LED emitter with a wavelength of 1650 nm is used [13], whose light will be absorbed by the glucose sample in a 3 ml quartz or acrylic cuvette as the case may be. This absorbance depends directly on the molecule of water and glucose; the higher the glucose concentration, the higher the absorption and vice versa. This absorbance will be detected by means of a photodiode, which converts the light signal (absorbance) into a small electric current that corresponds to the concentration of glucose in the sample [14]. 4 photodiodes were used: diameter active area of 0.06 mm, 0.5 mm, 1 mm, and 1.5 mm, respectively [15–18]. A transimpedance amplifier is used, as shown in Figure 5. This circuit converts the current signal from the photodiode to a voltage signal to be easily manipulated in the conditioning stages [19].

2.4. Signal Conditioning

2.4.1. *Low-Pass Filter.* A second-order Butterworth-type low-pass filter with 1 Hz cutoff frequency and Sallen-Key topology is utilized to attenuate signals undesirable high-frequency that are found present in the glucose-related signal; the circuit diagram is shown in Figure 6. The components selection was based on the calculation for the active



FIGURE 3: Extraction of blood plasma.

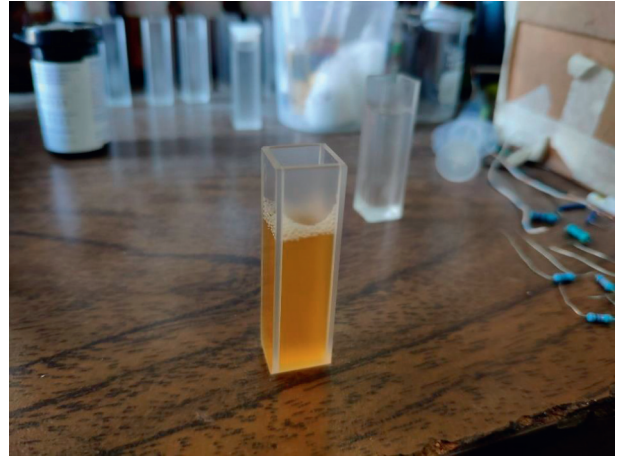


FIGURE 4: Blood plasma deposited in the quartz cuvette.

filters using equations (11) and (12) described in [20], where C_1 , C_2 , and R are the capacitors and resistance of the active filter, respectively, Q is the quality factor of the filter, and f_c is the cutoff frequency.

$$C_1 = \frac{2Q}{2\pi f_n R}, \quad (11)$$

$$C_2 = \frac{1}{4\pi f_n Q R}. \quad (12)$$

TABLE 2: Concentrations used for preparing samples of blood plasma solutions.

Samples (mg/dl)	Blood plasma (ml)	Solution DX-5, Pisa (μ l)
100	3	0
200	3	62.5
300	3	127.7
400	3	195.7
500	3	266.7
600	3	341
700	3	418.7
800	3	500
900	3	585.4
1000	3	675

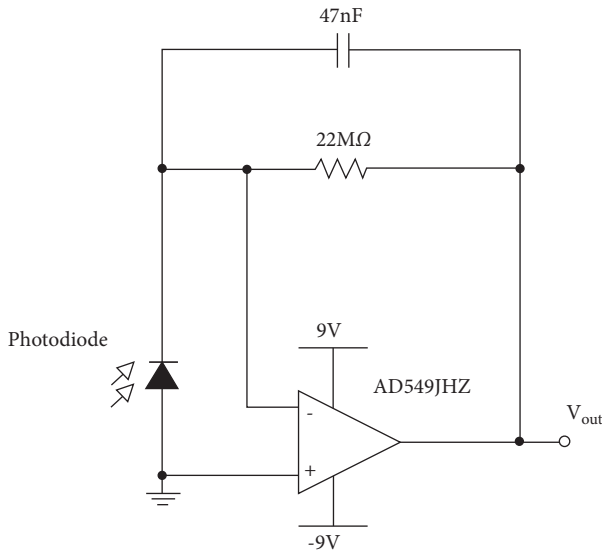


FIGURE 5: Transimpedance amplifier.

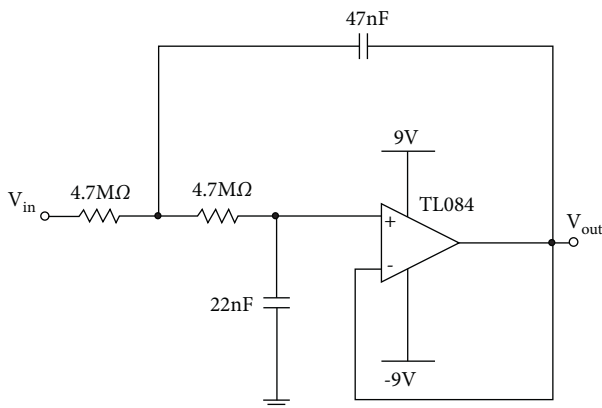


FIGURE 6: Low-pass filter Butterworth.

2.4.2. *Instrumentation Amplifier.* An AD620 is used to amplify glucose-related signal as shown in Figure 7; a gain of 2 is selected according equation (13) described in [21], where R_g is the gain resistance and G is the gain of amplifier.

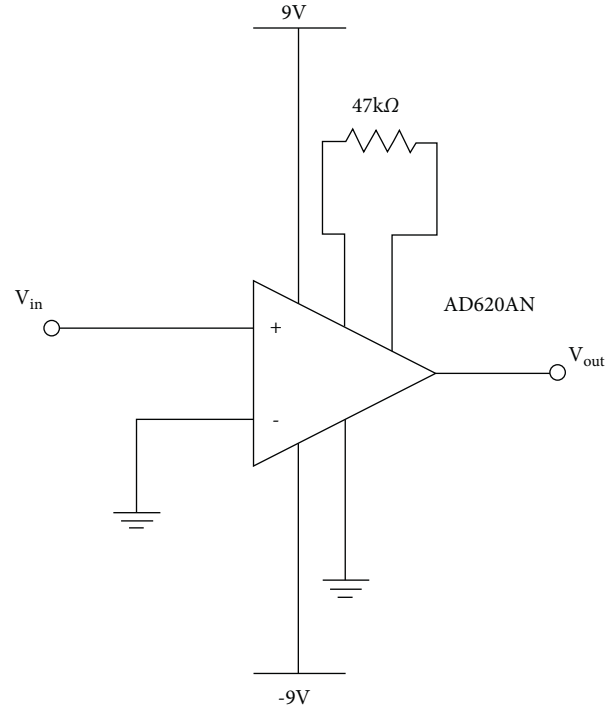


FIGURE 7: Instrumentation amplifier.

$$R_g = \frac{49400\Omega}{G - 1}. \quad (13)$$

2.4.3. *Low-Pass Filter.* In this stage is used the low-pass filter of Figure 6.

3. Results

A downward pattern is noticed; as the glucose concentration in the solution increases, the voltage output decreases. The results demonstrated a more downward voltage pattern when using a quartz cuvette and a less downward pattern in an acrylic cuvette, as given in Table 3. Greater intensity light is detected by the receiving circuit obtaining a greater sensitivity between each variation of the glucose concentration. The voltage decrease average using an acrylic cuvette was 7.5 mV and 10.9 mV for a quartz cuvette.

Figure 8 shows a comparison between acrylic cuvette and quartz cuvette. 1 volt was used as the initial reference value using the average voltage decrement, respectively. In this figure, a greater sensitivity can be observed when using a quartz cuvette.

Table 4 provides the voltage decrease averages for each active area.

The results showed that in order to obtain a greater sensitivity to glucose, it is not only the cuvette material that matters but also the active area of the photodiode, meaning the greater the active area, the greater the downward voltage pattern (sensitivity). Table 5 provides the voltage decrement values of each active area, respectively.

TABLE 3: Downward voltage pattern using acrylic and quartz cuvettes.

Glucose concentration (mg/dl)	Voltage using acrylic cuvette (V)	Decrease using acrylic cuvette (mV)	Voltage using quartz cuvette (V)	Decrease using quartz cuvette (mV)
0	2.233	NA	3.253	NA
100	2.224	9	3.245	8
200	2.212	12	3.235	10
300	2.205	7	3.224	11
400	2.198	7	3.212	12
500	2.189	9	3.205	7
600	2.186	3	3.191	14
700	2.182	4	3.182	9
800	2.169	13	3.169	13
900	2.166	3	3.155	14
1000	2.158	8	3.144	11

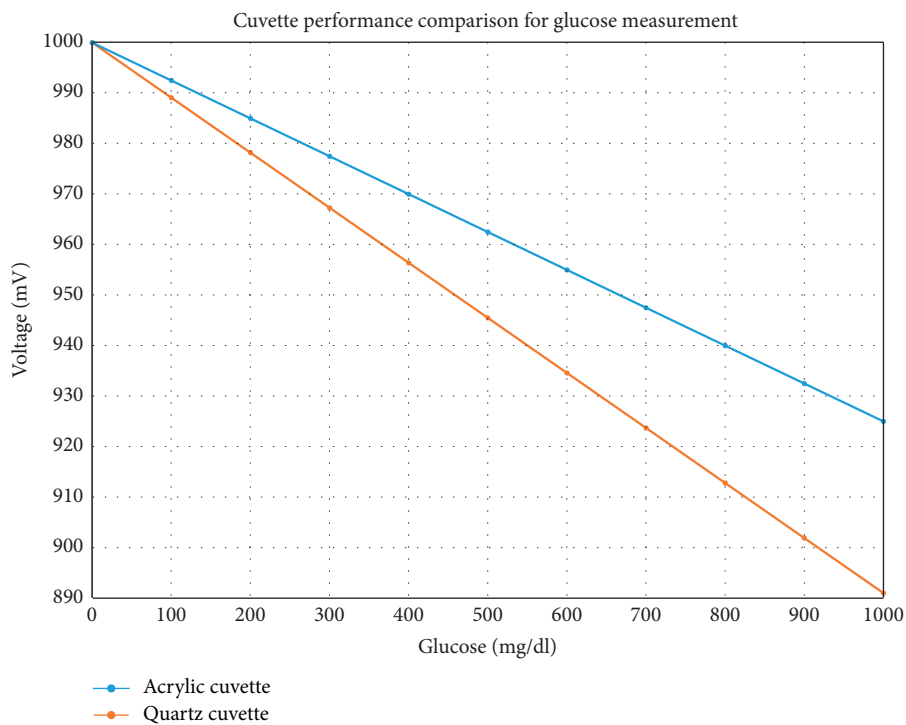


FIGURE 8: Cuvette performance comparison for glucose measurement.

TABLE 4: Average downward voltage pattern.

Active area (mm)	Average downward voltage pattern (mV)
1.5	10.9
1	4.1
0.5	1.9
0.06	0.06

TABLE 5: Glucose measurement using active area of 1.5, 1, 0.5, and 0.06 mm.

Glucose concentration (mg/dl)	Voltage using 1.5 mm active area (V)	Decrease using 1.5 mm active area (mV)	Voltage using 1 mm active area (V)	Decrease using 1 mm active area (mV)	Voltage using 0.5 mm active area (mV)	Decrease using 0.5 mm active area (mV)	Voltage using 0.06 mm active area (mV)	Decrease using 0.06 mm active area (mV)
0	3.253	NA	1.391	NA	443	NA	20	NA
100	3.245	8	1.386	5	441	2	19.9	0.1

TABLE 5: Continued.

Glucose concentration (mg/dl)	Voltage using 1.5 mm active area (V)	Decrease using 1.5 mm active area (mV)	Voltage using 1 mm active area (V)	Decrease using 1 mm active area (mV)	Voltage using 0.5 mm active area (mV)	Decrease using 0.5 mm active area (mV)	Voltage using 0.06 mm active area (mV)	Decrease using 0.06 mm active area (mV)
200	3.235	10	1.383	3	437	4	19.7	0.2
300	3.224	11	1.378	5	436	1	19.7	0
400	3.212	12	1.371	7	434	2	19.7	0
500	3.205	7	1.367	4	431	3	19.6	0.1
600	3.191	14	1.362	5	430	1	19.6	0
700	3.182	9	1.36	2	428	2	19.5	0.1
800	3.169	13	1.356	4	427	1	19.5	0
900	3.155	14	1.353	3	426	1	19.4	0.1
1000	3.144	11	1.35	3	424	2	19.4	0

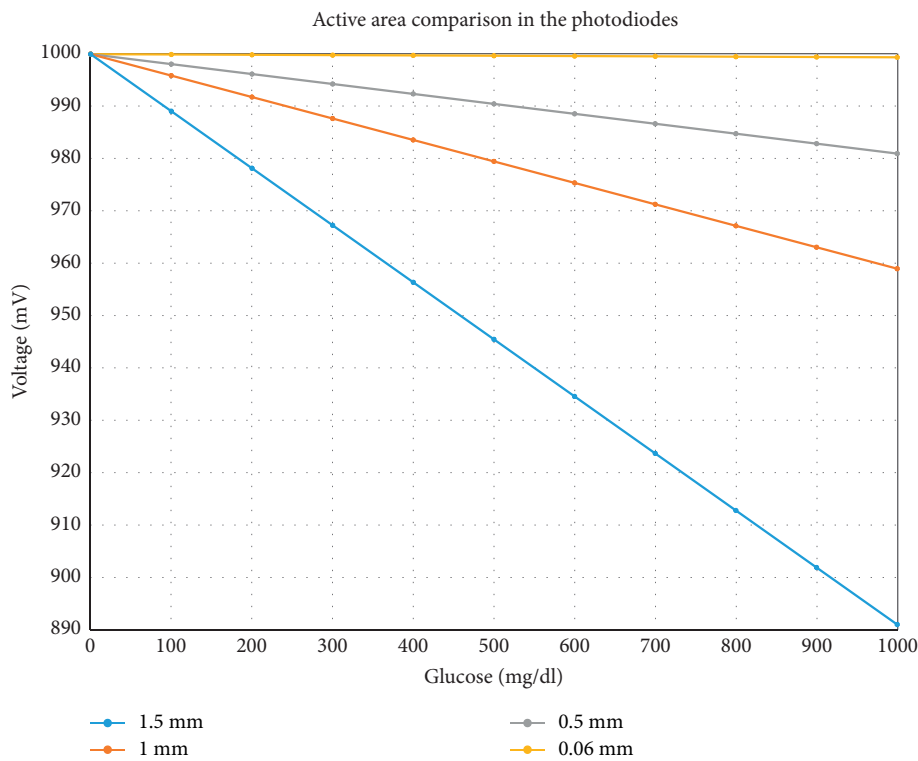


FIGURE 9: Active area comparison in the photodiodes.

Figure 9 shows a comparison between the active areas of each photodiode. 1 volt was used as the initial reference value using the average voltage decrease value, respectively.

Figure 10 shows the downward voltage pattern at the photodiode of 1.5 mm due to plasma glucose concentration. The results obtained were a greater average downward voltage pattern in plasma than in water, as given in Table 6. This occurs because water and glucose share absorption bands, and water directly interfere with glucose measurement [12]. The experimental results showed that the plasma does not contain water in its entirety, as indicated in [22], which means that the fewer the water molecules are in a glucose solution, the greater the decrease in voltage between each concentration and consequently the greater the sensitivity to glucose.

For glucose measurement, 3 samples of human blood plasma with a concentration of 100 mg/dl were used. The blood glucose level of plasma donors is measured with a commercial glucometer One Touch Ultra Mini. The requirement is that the glycemic value is 100 mg/dl. The results are given in Table 7.

4. Discussion

The sensitivity to glucose is directly related to the active area of the photodiode and the material of the cuvette. The comparison between cuvette materials and active area represents a higher average downward voltage pattern between each glucose concentration. This comparison allows

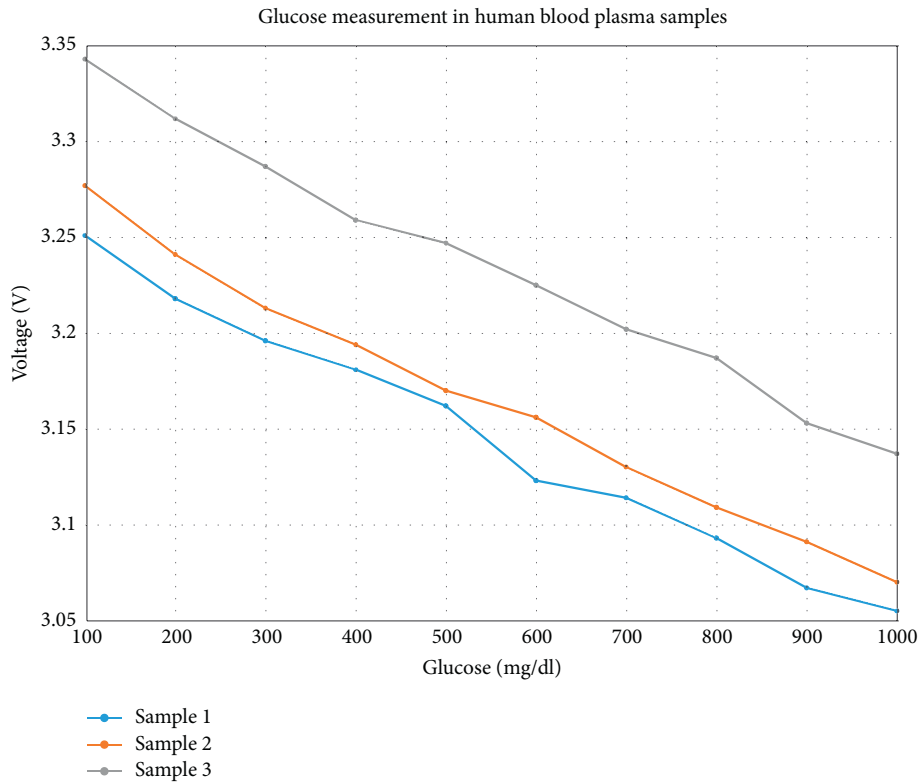


FIGURE 10: Glucose measurement in human blood plasma solutions.

TABLE 6: Comparison of the average downward voltage pattern between water and plasma.

Solvent	Average downward voltage pattern (mV)
Water	10.9
Blood plasma	22.5

TABLE 7: Glucose measurement in human blood plasma samples 1, 2, and 3.

Glucose concentration (mg/dl)	Voltage using sample 1 (V)	Decrease using sample 1 (mV)	Voltage using sample 2 (V)	Decrease using sample 2 (mV)	Voltage using sample 3 (V)	Decrease using sample 3 (mV)
100	3.251	NA	3.277	NA	3.343	NA
200	3.218	33	3.241	36	3.312	31
300	3.196	22	3.213	28	3.287	25
400	3.181	15	3.194	19	3.259	28
500	3.162	19	3.17	24	3.247	12
600	3.123	39	3.156	14	3.225	22
700	3.114	9	3.13	26	3.202	23
800	3.093	21	3.109	21	3.187	15
900	3.067	26	3.091	18	3.153	34
1000	3.055	12	3.07	21	3.137	16

to know the necessary conditions to obtain a higher sensitivity that does not require an increase in the gains in the amplifiers. Using a 1.5 mm active area and a quartz cuvette gives a sensitivity of 0.225 mV per 1 mg/dl of glucose concentration. On the other hand, when blood plasma is used, water does not interfere with glucose measurements.

5. Conclusions

In conclusion, the experimental tests showed that when designing a glucose meter using the near infrared technique, a photodiode with a larger active area and quartz material for the cuvette should be considered. The design of this blood

plasma glucose meter shows good linearity, having an R^2 of 0.99 and a sensitivity of 0.225 mV per 1 mg/dl of glucose. A noninvasive blood glucose meter could be designed, either on a finger or on another part of the body with the previously mentioned parameters. It is important to consider the difference in voltage readings at the beginning of each repetition of samples since the largest difference is between samples 1 and 3, being 92 mV, and the smallest difference is between samples 2 and 1, being 26 mV, although the downward voltage pattern remains the same for each of the samples.

Data Availability

The data used to support the findings of this study are included within the article.

Conflicts of Interest

The authors declare that there are no conflicts of interest.

References

- [1] WHO, *Diabetes Disease*, WHO, Geneva, Switzerland, 2020, <https://www.who.int/news-room/fact-sheets/detail/diabetes>.
- [2] WHO, *Noncommunicable Diseases*, WHO, Geneva, Switzerland, 2018, <https://www.who.int/news-room/fact-sheets/detail/noncommunicable-diseases>.
- [3] A. Katsarou, S. Gudbjörnsdóttir, A. Rawshani et al., "Type 1 diabetes mellitus," *Nature Reviews Disease Primers*, vol. 3, no. 1, p. 17016, 2017.
- [4] R. A. DeFronzo, E. Ferrannini, L. Groop et al., "Type 2 diabetes mellitus," *Nature Reviews Disease Primers*, vol. 1, no. 1, p. 15019, 2015.
- [5] N. G. Forouhi and N. J. Wareham, "Epidemiology of diabetes," *Medicine*, vol. 47, no. 1, pp. 22–27, 2019.
- [6] W. Villena Gonzales, A. Mobashsher, and A. Abbosh, "The progress of glucose monitoring—a review of invasive to minimally and non-invasive techniques, devices and sensors," *Sensors*, vol. 19, no. 4, p. 800, 2019.
- [7] L. A. Castro-Pimentel, A. D. C. Tellez-Anguiano, O. M. Guerra-Alvarado, and K. R. Hernandez-Franco, "Non-invasive glucose measurement using spectrography in near infrared (NIR)," *IEEE Latin America Transactions*, vol. 17, no. 11, pp. 1754–1760, 2019.
- [8] S. Vashist, "Continuous glucose monitoring systems: a review," *Diagnostics*, vol. 3, no. 4, pp. 385–412, 2013.
- [9] K. B. Beć and C. W. Huck, "Breakthrough potential in near-infrared spectroscopy: spectra simulation. A review of recent developments," *Frontiers of Chemistry*, vol. 7, p. 48, 2019.
- [10] W. Mäntele and E. Deniz, "UV–VIS absorption spectroscopy: Lambert-Beer reloaded," *Spectrochimica Acta Part A: Molecular and Biomolecular Spectroscopy*, vol. 173, pp. 965–968, 2017.
- [11] J. H. Hardesty and B. Attili, *Spectrophotometry and the Beer-Lambert Law: An Important Analytical Technique in Chemistry*, Collin College, Department of Chemistry, McKinney, TX, USA, 2010.
- [12] K. Maruo and Y. Yamada, "Near-infrared noninvasive blood glucose prediction without using multivariate analyses: introduction of imaginary spectra due to scattering change in the skin," *Journal of Biomedical Optics*, vol. 20, no. 4, p. 047003, 2015.
- [13] Marktech-Optoelectronics, *MTE5116N-WRC*, <https://www.marktechopto.com/pdf/products/DataSheet/MTE5116N-WRC.pdf>.
- [14] B. Mishra, K. Sharma, and P. Choudhary, "A low noise op-amp transimpedance amplifier for InGaAs photodetectors," *International Research Journal of Engineering and Technology*, vol. 2, pp. 54–58, 2015.
- [15] Advanced-Photonix, *SD0003-3111-111*, <https://media.digikey.com/pdf/Data%20Sheets/Photonic%20Detectors%20Inc%20PDFs/SD0003-3111-111.pdf>.
- [16] Advanced-Photonix, *SD0200-3111-111*, <https://media.digikey.com/pdf/Data%20Sheets/Photonic%20Detectors%20Inc%20PDFs/SD0200-3111-111.pdf>.
- [17] Advanced-Photonix, *SD039-151-011*, <https://media.digikey.com/pdf/Data%20Sheets/Photonic%20Detectors%20Inc%20PDFs/SD039-151-011.pdf>.
- [18] Marktech-Optoelectronics, *MTPD1346D-150*, <https://www.marktechopto.com/pdf/products/datasheet/MTPD1346D-150.pdf>.
- [19] B. Razavi, "The transimpedance amplifier [a circuit for all seasons]," *IEEE Solid-State Circuits Magazine*, vol. 11, no. 1, pp. 10–97, 2019.
- [20] T. Deliyannis, Y. Sun, and J. K. Fidler, *Continuous-Time Active Filter Design*, CRC Press, Boca Raton, FL, USA, 2019.
- [21] Analog-devices, *AD620*, <https://www.analog.com/media/en/technical-documentation/data-sheets/AD620.pdf>.
- [22] M. Brust, C. Schaefer, R. Doerr et al., "Rheology of human blood plasma: viscoelastic versus Newtonian behavior," *Physical Review Letters*, vol. 110, Article ID 078305, 2013.